LASER INTERFEROMETER GRAVITATIONAL WAVE OBSERVATORY
- LIGO -

Document Type	LIGO-T970156-03 - D	3/17/98

LIGO Cavity Lengths and Modulation Frequencies

David Tanner

Distribution of this draft:

Detector

This is an internal working note
of the LIGO Project..

University of Florida
Department of Physics, LIGO Group
Gainesville, FL 32611-8440

TABLE OF CONTENTS

LIGO cavity lengths and modulation frequencies

D.B. Tanner

Department of Physics, University of Florida, Gainesville, FL 32611-8440, USA

The lengths of the mode cleaner (L_{mc}) and of the recycling cavity (L_{rc}) in LIGO are considered in light of constraints imposed by existing vacuum chamber dimensions. The optimum lengths, and corresponding modulation frequencies, are given in the following table. Here, f_{res} is the frequency of a modulation that produces sidebands resonant in the recycling cavity but not the interferometer arms. f_{nr} is the frequency of a modulation that is not resonant in either. Both sets of sidebands must resonate in the mode cleaner.

IFO	L_{mc} (mm)	L_{rc} (mm)	f_{res} (MHz)	f_{nr} (MHz)
4-km	12240	9188	24.493	61.232
2-km	15251	12715	29.486	68.800

Gainesville, 20 October 1998

A. Introduction

This note is one of a series of memos about baseline lengths for the mode cleaner and recycling cavity, along with the corresponding RF modulation frequencies. The series includes work by M. Zucker and P. Fritschel,[1] myself,[2] and Dennis Coyne.[3] The baseline RF frequencies are listed in the Detector Subsystem Requirements[4] and in the IOO Conceptual Design document.[5] They are 24.0 MHz for the 4-km interferometer and 32.1 MHz for the 2-km interferometer.

In the current phase of the input optics (IOO) design these lengths and nominal frequencies are refined, as described in this note.

B. Relation between lengths and modulation frequencies

The core optics of LIGO employ two modulation frequencies:

1. The first modulation frequency gives upper and lower sidebands that are resonant in the recycling cavity but not resonant in the interferometer arm cavities. These are used for controlling the lengths of the interferometer and for aligning the arm cavities and the beam splitter.
2. The second gives upper and lower sidebands that are not resonant in the recycling cavity. These are used for alignment of the recycling mirror.

The values of these frequencies are set by the lengths of the respective cavities, according to the usual Fabry-Perot conditions.

The resonant sideband frequency must satisfy

$$f_{res} = \frac{(k + 1/2)c}{2L_{rc}}, \tag{1}$$

where ($k = 0,1,2 \ldots$) and L_{rc} is the recycling cavity length. The extra factor of $1/2$ occurs because the carrier is resonant in the arm cavities whereas the sidebands are *not* resonant in the arms, giving a extra 180° phase shift in the reflectivity of the arms.

The nonresonant sideband frequency is chosen to be far from the recycling cavity resonances. A reasonable condition is that the frequency offset be several times the width of the resonance, so that the phase shift on reflection be close to 0.

Both the resonant and nonresonant sidebands must be equal to one of the mode cleaner resonances, because the RF modulation is imposed before the mode cleaner. The resonant frequencies of the mode cleaner are:

$$f_{mc} = \frac{nc}{2L_{mc}}, \tag{2}$$

where n is an integer (1,2,3 ...) and L_{mc} the mode cleaner length.* The frequencies f_{mc} and f_{res} must equal each other because the sidebands are resonant simultaneously in both the mode cleaner and the recycling cavity.

The remaining consideration in choice of the modulation frequencies is that they must miss all the harmonics of the arm free spectral range: 37.5 kHz in the 4-km instrument; 75 kHz in the 2-km instrument.

C. Constraints affecting modulation frequencies

1. Vacuum chambers

The mode cleaner and recycling cavities span vacuum chambers whose separations determine the cavity lengths. There is some flexibility on account of the size of the optical tables in these chambers. The mode cleaner for the 4-km instrument occupies HAM-1 and HAM-2; the interferometer recycling mirror is in HAM-3; the input test masses are in BSC-1 and BSC-3. The mode cleaner for the 2-km instrument occupies HAM-7 and HAM-8; the recycling mirror is in HAM-9; the input test masses are in BSC-7 and BSC-8. Table 1 gives some details.

Table 1. Dimensions of vacuum chambers in LIGO, in mm.

Item			
	HAM table length, L_{HAM}	1905	
	HAM table width, W_{HAM}	1702	
	BSC table length,† L_{BSC}	931	
	BSC table width,† W_{BSC}	845	
IFO		Min	Max
Both	HAM-1(7) to HAM-2(8) (Mode Cleaners)	11816	15626
4-km	HAM-3 to BSC-1/3 (Recycling Cavity)	6890	9726
2-km	HAM-9 to BSC-7/8 (Recycling Cavity)	11530	14366

† The BSC tables are 1257 mm in diameter; I've taken the size as the included rectangle whose width is the distance between the outsides of the large optics suspensions (LOS) on these tables.

The Min and Max dimensions in Table 1 must be adjusted by several factors to estimate

* The length is *half* the round-trip length of the cavity. For a triangular-mode cleaner, in the shape of a tall isosceles triangle, it is then half the base plus the length from base corner to apex.

the minimum and maximum path lengths in mode cleaner and recycling cavities. These adjustments are listed in the following sections.

2. Mode cleaner

The mode cleaner is sketched in Fig. 1, with some key dimensions marked. The factors governing the optical length of the mode cleaner include the following items:

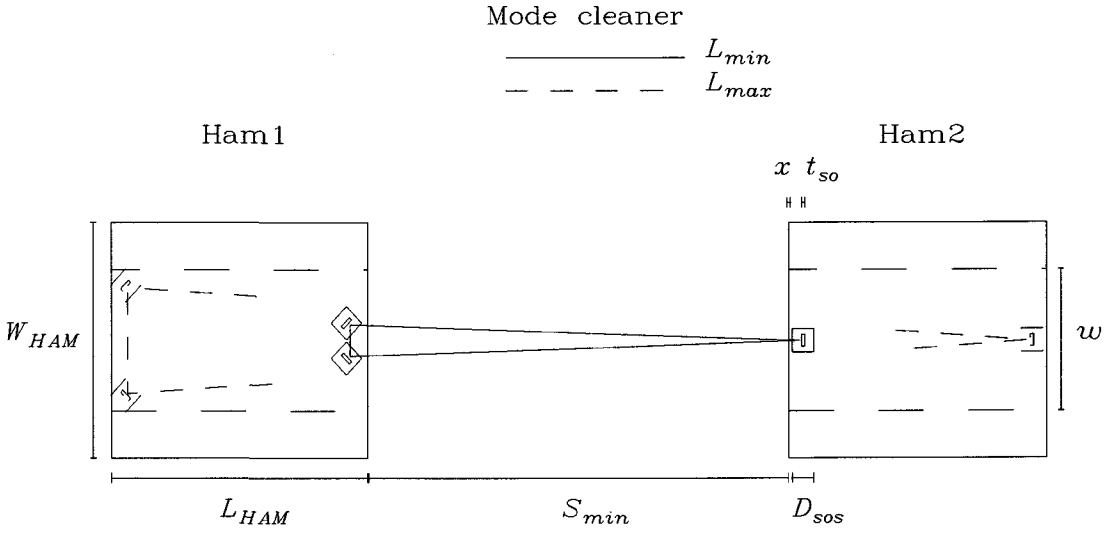

Fig. 1. The mode cleaner. The tables are shown approximately 4× enlarged in size, with the suspension bases and mirror thicknesses roughly to the scale of the tables. The minimum length is shown as the solid line; the maximum as dashed lines.

1. S^{mc}_{min} is the minimum table separation and S^{mc}_{max} is the maximum table separation, from Table 1.
2. The curved mirror must be moved away from the edge of the table so that the small optics suspension (*sos*) does not overhang the table. The distance from mirror face to table edge is half the depth of the suspension (D_{sos}) adjusted by half the thickness of the optic (t_{so}). (If the mirror is near the back edge—from its point of view—there must be space behind it for a length/alignment sensing pickoff. See point 7, below.)
3. The flat mirrors are at nearly 45° to the table edge, so their centers need to be moved away by $\sqrt{2}/2$ of D_{sos}, with an adjustment for the thickness of the mirror $[(\sqrt{2}/2)t_{so}]$.
4. The base b of the triangular beam path in the mode cleaner must be included in the optical path length. The minimum base size is set by having the corners of the small

optics suspension almost touching. It might seem that the maximum could be set by using the full 1702 mm width W_{HAM} of the HAM chamber table, less the $(\sqrt{2}/2)D_{sos}$ needed to keep each suspension fully on the table. However, the beam tube joining HAM-1 and HAM-2 is only 775 mm in diameter, and this tube also must accommodate the large beam from the IOO telescope. Thus, I have used half the tube diameter, 387 mm for the available width, w. (This also allows space on the HAM tables for beam expanders and steering mirrors.)

5. Both the minimum and the maximum size for b are adjusted for the thickness of the mirror.
6. There is another adjustment because the long sides of the triangular path are not parallel to the axis, and so are longer by approximately $b^2/8S$. This quantity is $\approx$1 mm when the base equals its maximum value, and even more negligible when the base is near its minimum.
7. The mode cleaner need a certain amount of space A_{ux} around it to allow for the extraction of auxillary beams. This distance includes space for a mirror behind the spherical mirror and for beam steering mirrors near the two flats.[6] This space takes away from the maximum length of the mode cleaner.
8. There probably should be a small gap x between the suspensions and between the actual table edge, in the cases where the suspensions approach the edge, to allow for chamfers or lips at the edge introduced by the machining process.

From the above, I arrive at the following equations for the effective optical path lengths in the mode cleaner.

Minimum:

$$L^{mc}_{min} = S^{mc}_{min} + \frac{1+2\sqrt{2}}{2}(D_{sos} - t_{so}) + 3x \tag{3}$$

Maximum:

$$L^{mc}_{max} = S^{mc}_{max} - \frac{1+2\sqrt{2}}{2}(D_{sos} + t_{so}) - 2A_{ux} - 2x + \frac{1}{2}w + \frac{w^2}{8S^{mc}_{max}} \tag{4}$$

3. Effect of Schnupp asymmetry and beam offsets

LIGO uses Schnupp or frontal modulation in its length-sensing and alignment system.[7,8] The basic idea is to introduce an asymmetry between the Michelson arms. When the carrier is exactly at a dark fringe, the modulation sidebands will be slightly away from a dark fringe, so that some sideband power is sent by the interferometer into the output port. This

power generates signals used in the beam splitter and input test mass locking scheme. The baseline design for LIGO uses an asymmetry* of $S_s = 250$ mm.[4] Finally, so far as the effective recycling cavity length for the RF modulation goes, it is the *average* length of the recycling cavity that matters.

Both the 4-km and the 2-km interferometer have their optical centerlines displaced from the centerlines of the beam tubes. Because of this offset, the placement of the beam splitter may affect the Michelson and recycling cavity path length by making a difference between the y optical path and the x optical path. It is possible to use this difference to minimize the impact of the Schnupp offset on the range of motion of the input test masses.

a. 4-km interferometer

The 4-km interferometer has its optical centerline displaced (by $B_{off} = 200$ mm) from the centerlines of the beam tubes. Because of this offset, the placement of the beamsplitter affects the Michelson and recycling cavity path length, as sketched in Fig. 2, below. In this figure, the x and y coordinates intersect at the center of the beamsplitter chamber. If the beamsplitter is in the second or fourth quadrant, the y physical length will be shorter or longer than the x physical length by $2B_{off}$. If the beamsplitter is in the first or third quadrant, the offset has no effect on length. In the present design, the beamsplitter is in

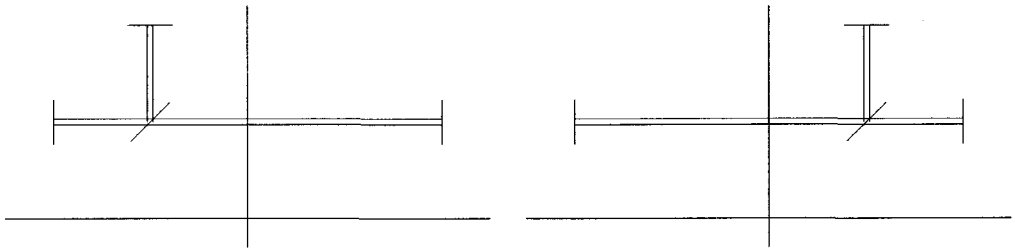

Fig. 2. Recycling cavity in the 4-km interferometer illustrating the effect of beamsplitter placement on Michelson optical path lengths. In each drawing the recycling mirror is on the left and the x and y input test masses are on the right and top, respectively. These are the same distance along the centerline from the origin. The beamsplitter is displaced from the origin; it in the second quadrant in the left drawing and the first quadrant on the right. The asymmetry in path lengths in the left drawing is evident.

* Note that there are three possible definitions for this quantity: (1) the optical path difference, (2) the difference in physical lengths, (3) the amount each mirror is moved from the equal-path-difference location. According to the Detector Subsystem Requirements document,[4] the maximum Schnupp distance of 250 mm refers to 1/2 the physical difference in lengths, *i.e.*, option (3) above. In this case, the optical path difference is 1 m.

the second quadrant, giving an asymmetry in the paths. The beam along x goes the same distance as if it were on the centerline; the beam along y turns a distance B_{off} before it reaches the y axis, and starts parallel to y from a point B_{off} above the x axis.

With the Schnupp offset included, the remaining asymmetry in placement of the input test masses is

$$A_{symm} = |B_{off} - S_s|. \tag{5}$$

(This is defined in the same way as the Schnupp offset, *i.e.*, as 1/2 the physical difference in lengths if the ITM's are placed in identical positions on the tables.)

b. 2-km interferometer The layout of the 2-km interferometer is shown in Fig. 3. This instrument also has its optical centerline displaced (by $B_{off} = 200$ mm) from the centerlines of the beam tubes. In addition, the 2-km interferometer is folded into the beam tubes by

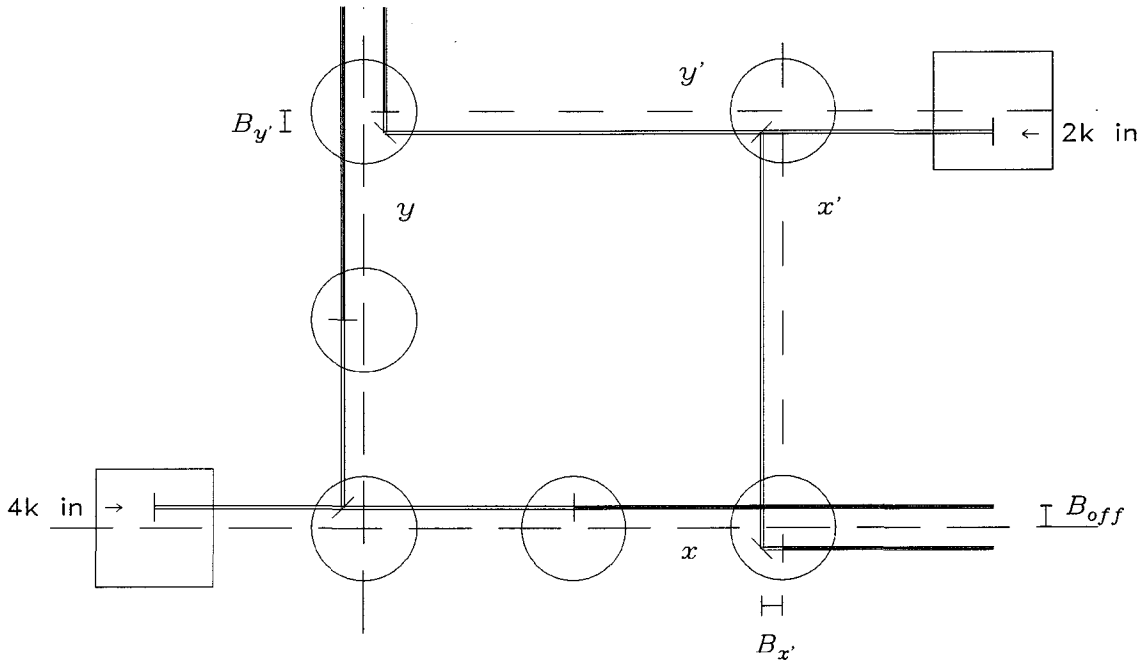

Fig. 3. Optical layout of the core optics. The coordinate systems are shown as dashed lines, crossing in the two beamsplitter chambers. Both interferometers have their beams offset from the centerline by B_{off}. The 2-km beam enters in the upper right. The 2-km beamsplitter directs the beam parallel to the x' and y' axes. The offsets $B_{x'}$ and $B_{y'}$ are shown. Turning mirrors direct the beam into the arm cavities. The recycling mirrors and input test masses are shown as small dashes, centered in their chambers.

turning mirrors located in the same BSC's as the input test masses. These turning mirrors have two consequences: (1) They take up space in the chamber, reducing the range of motion of the ITM's. (2) Their placement, coupled with the beamsplitter location, gives some additional adjustability in the x and y path lengths.

The 2-km interferometer has an asymmetry given by

$$A_{symm} = |B_{off} - B_{y'} + B_{x'} - S_s|, \tag{6}$$

where $B_{x'}$ and $B_{y'}$ are the offsets of the beams from the tube centerlines along the paths between the beamsplitter and the turning mirrors.

4. Recycling cavity

The recycling cavity is sketched in Fig. 4, with some key dimensions marked. The factors governing the optical length of the recycling cavity include the following items:

1. S_{min} is the minimum table separation and S_{max} is the maximum table separation, from Table 1.

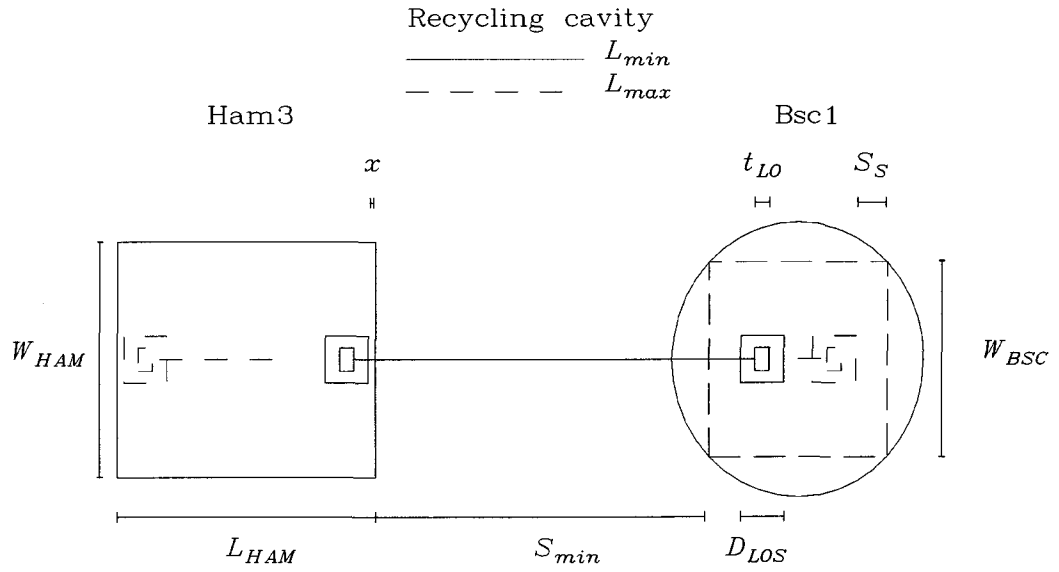

Fig. 4. The recycling cavity. The tables are shown approximately 4× enlarged in size with the suspension bases and mirror thicknesses roughly to the scale of the tables. The minimum length is shown as the solid line; the maximum as dashed lines. The Schnupp offset prevents the average location of the input test mass from being moved to the edges of the table.

2. The average position of the input test masses must be moved away from the table edge by the remaining asymmetry, which is given in Eqs. 5 and 6, above.

3. The mirrors must be moved away from the edge of the table so that the large optics suspensions (LOS) do not overhang the table. The distance from mirror face to table edge is half the depth of the suspension (D_{LOS}). Note that the recycling mirror faces the cavity, but the input test mass reflective surface faces *away* from the cavity, so that the offsets from the thickness of the optic cancel.

4. There needs to be an adjustment for the extra optical path in the substrate of the input test mass, $(n-1)t_{LO}$, where n is the refractive index.

5. There is also an adjustment for the additional path in the beam splitter (including the effects of refraction), δt_{BS}. With a little bit of trigonometry and Snell's law, I get the neat result

$$\begin{aligned} \delta t_{BS} &= t_{BS}\left(\sqrt{n^2 - \sin^2\theta_i} - \cos\theta_i\right) \\ &= t_{BS}\left(\sqrt{n^2 - \frac{1}{2}} - \sqrt{\frac{1}{2}}\right) \qquad \text{with } \theta_i = 45^\circ \end{aligned} \tag{7}$$

   where θ_i is the angle of incidence and t_{BS} the beam-splitter thickness.

6. There probably should be a small gap x between the suspensions and the actual table edge, to allow for chamfers or lips at the edge introduced by the machining process.

7. In the 2-km interferometer, space must be left for the turning mirrors. With a little geometry, I find that this increases the minimum path length by

$$F = \frac{L_{BSC}}{2} - \min(B_{x'}, B_{y'}) + \frac{D_{LOS} + W_{LOS} - t_{LO}}{\sqrt{8}}. \tag{8}$$

8. In the 4-km interferometer, of course, $F = 0$.

From this I come to the following equations for the effective optical path lengths in the recycling cavity.

Minimum:

$$L^{rc}_{min} = S^{rc}_{min} + A_{symm} + D_{LOS} + 2x + (n-1)t_{LO} + \delta t_{BS} + F \tag{9}$$

Maximum:

$$L^{rc}_{max} = S^{rc}_{max} - A_{symm} - D_{LOS} - 2x + (n-1)t_{LO} + \delta t_{BS} \tag{10}$$

D. Arm resonances

I have considered briefly the interrelation of the arm-cavity resonances and the recycling cavity resonances. The arm-cavity resonances occur at:

$$f_{arm} = \frac{\ell c}{2L_{arm}}, \tag{11}$$

where $L_{arm} = \{4, 2\}$ km and ℓ is an integer. The frequency separation of these resonances is 37.5 kHz for the 4-km interferometers, and 75 kHz for the 2-km interferometer. When the length of the arms is resonant with the carrier signal, the sidebands must fail to resonate in the arms, *i.e.*, $f_{res} \neq f_{arm}$. However, the arms should not be maximally antiresonant, in order to keep the second-order sidebands from resonating in the arm cavities.[9] I have adjusted the calculations below to move the modulation frequencies 4–6 kHz away from the maximmally antiresonant values. Typically, to make the arm cavities adequately nonresonant requires a length change of about 2 mm in the mode cleaner and recycling cavity lengths, and changes the resonant modulation frequency by a few kHz. Note that it takes a length change of about 6000 mm in arm-cavity length to move the sidebands from the ℓ^{th} arm resonance to the $\ell \pm 1^{\text{st}}$ arm resonance. Since 3m of motion is probably not available in the positioning of the test masses, it will most likely be the responsibility of the mode-cleaner and recycling cavities to avoid degeneracy with the arm cavities.

Displacement of the arm cavities from antiresonance leads to a phase change in the reflected sidebands $\Delta\phi$. This value is estimated in LIGO-T960181[9]; it is typically 0.01 radians. In turn, the recycling cavity must be increased in length by $\Delta\phi L_{rc}/(2k+1)\pi$, a value of 5–8 mm.

E. Numerical values

1. Dimensions used

Table 2 lists the quantities that come into the calculation and gives the values used. Using these numbers, I calculate the *optical lengths* for the interferometers, in Table 3. The range of lengths in Table 3 is somewhat less than those in Table 1.

2. Resonant sideband frequencies

Given the above range of lengths, it is then possible to find the range of frequencies for which *both* the mode cleaner and the recycling cavity resonance conditions (Eqs. 2 and 1) are satisfied. Several candidate length and modulation frequency ranges emerge. These are listed in Table 4, which should be compared to Table 3 of Ref. 1.

I also carried out an optimization in Excel to (1) adjust the mode cleaner length within the limits given in Table 3, (2) calculate the corresponding recycling cavity length, (3)

Table 2. Quantities affecting the optical lengths of the mode cleaner and recycling cavities. (All dimensions in mm.)

Item	Symbol	Value
Small optic suspension depth	D_{sos}	127
Small optic suspension width	W_{sos}	156
Small optic thickness	t_{so}	25
Space for auxillary mirrors	A_{ux}	105
Edge clearance	x	10
Beam tube limits on MC width	w	387
Large optic suspension depth	D_{LOS}	267
Large optic suspension width	W_{LOS}	445
Large optic thickness	t_{LO}	100
Beam-splitter thickness	t_{BS}	40
Offset in beam tube	B_{off}	200
2-km x' offset	$B_{x'}$	57
2-km y' offset	$B_{y'}$	161
Schnupp offset (nominal)	S_s	250
Schnupp offset (maximum, 4k)	S_s^{4k}	500
Schnupp offset (maximun, 2k)	S_s^{2k}	300
Turning mirror space in 2-km IFO	F	604
Refractive index	n	1.45

Table 3. Optical lengths in LIGO, in mm.

IFO		Min	Ave	Max	Range of motion
Both	Mode cleaner	12041	13671	15300	3259
4-km	Recycling cavity	7444	8375	9306	1862
2-km	Recycling cavity	12663	13327	13992	1329

assure that the recycling cavity was within limits, (4) optimize the lengths to center them within the allowable range, and (5) make small adjustments in length to make the resonant sideband adequately nonresonant in the arm cavities. This procedure leads to the suggested frequencies in Table 5, which should be compared to Table 1 of Ref. 3.

Table 4. Bounds for the 4k and 2k interferometers up to $n = 5$, $k = 5$. (All dimensions in mm.)

IFO	n, k	L_{mc}/L_{rc}	f (MHz)	L_{mc}	L_{rc}
4-km	1,0	2.0	9.80–10.07	14889–15300	7444–7650
	2,1	1.3333	24.16–24.90	12041–12408	9031–9306
	3,1	2.0	29.39–30.20	14889–15300	7444–7650
	4,2	1.6	40.27–49.80	12041–14889	7526–9306
	5,2	2.0	48.98–50.34	14889–15300	7444–7650
	5,3	1.4286	56.38–62.24	12041–13294	8429–9306
2-km	3,2	1.2	29.39–29.59	15196–15300	12663–12750
	4,3	1.1429	39.19–41.43	14472–15300	12663–13388
	4,4	0.8889	48.21–49.80	12041–12437	13546–13992
	5,4	1.1111	48.98–53.27	14070–15300	12663–13770
	5,5	0.9091	58.92–62.24	12041–12437	13245–13992

Table 5. Optimized modulation frequencies for resonant sidebands and corresponding optical lengths. (All dimensions in mm.)

IFO	n, k	Notes	f (MHz)	L_{mc}	L_{rc}
4-km	1,0	MC length 2× RC.	9.886	15163	7582
	2,1		24.569	12202	9152
	3,1	MC length 2× RC.	29.657	15163	7582
	4,2	Recycling mirror centered in chamber.	44.745	13400	8375
2-km	3,2		29.498	15245	12704
	4,3		40.204	14914	13050
	4,4		48.943	12251	13782

Several comments may be made about Tables 4 and 5:

1. Given the constraints I have used, it is not possible to get a 24.0 MHz modulation frequency for the 4-km interferometer.
2. Neither is there a solution at 32.1 MHz for the 2-km configuration.
3. The solutions $n, k = 2, 1$, with frequency 24.569 MHz (4-km), $n, k = 3, 2$, with frequency 29.498 MHz (2-km), correspond to the n, k parameters chosen in Refs. 1 and 3.
4. The 2-km interferometer has no solution below 28.391 MHz, although there is a close match at $n, k = 2, 1$ at 18.67 MHz frequency.

5. The $n, k = 1, 0$ and $n, k = 3, 1$ solutions for the 4-km interferometer, although good from the point of view of length flexibility are probably ruled out by the wish to avoid integer ratios of lengths.

6. From the point of view of the optical layout, the mode cleaner prefers to be a little bit larger (say 500 mm larger) than its minimum size. (If it is right at either extreme, there is no chance to play off base size with height; if it tends towards its maximum size, it eats up real estate in HAM-1.)

3. Comparison to LIGO-T970068-00-D

As already mentioned, the $n, k = 2, 1$ (4-km) and $n, k = 3, 2$ (2-km) correspond to the n, k parameters chosen in Refs. 1 and 3. The first two lines of Table 6 compares the numbers in Table 5 with those in Ref. 3. The results are very close.

The lengths in Ref. 3 were obtained graphically using a CAD program, and there were no constraints that the modulation frequencies be antiresonant with the arm cavities. The third line shows the modification to those lengths if this constraint is imposed. The freqeuncies are changed by about 30 kHz (4-km) and 37 kHz (2-km) when this is done, with corresponding changes in length. I recommend choosing these values for the instrument.

Table 6. Comparison with previous results for frequencies and lengths. (All dimensions in mm.)

IFO	n, k	Notes	f (MHz)	L_{mc}	L_{rc}
4-km	2,1	LIGO-T970068-00-D	24.463	12255	9191
	2,1	Table 5	24.569	12202	9152
	2,1	Reoptimized LIGO-T970068-00-D	24.493	12240	9188
2-km	3,2	LIGO-T970068-00-D	29.449	15270	12725
	3,2	Table 5	29.498	15245	12704
	3,2	Reoptimized LIGO-T970068-00-D	29.486	15251	12715

4. The nonresonant sidebands

One has not a lot of flexibility with regard to the nonresonant sidebands. They must satisfy Eq. 2 but with a *different* mode cleaner resonance, $n' \neq n$. Moreover, in order to reduce the effects of "sidebands on sidebands" associated with series phase modulation of the laser, the nonresonant sidebands should be as large as possible compared to the resonant sidebands, at least $> 2\times$ them. Finally, because the Pockels cell produces harmonics at multiples of the modulation frequency, integer ratios of frequencies should be avoided.

a. 4-km interferometer

If 24.569 MHz ($n = 2$) is chosen for the resonant sideband frequency, one may in use 61.232, 85.725, 110.218 ... MHz for the nonresonant sidebands. This leads to 61.232 MHz ($n' = 5$) as the likely nonresonant sideband modulation frequency.

b. 2-km interferometer

If 29.498 MHz ($n = 3$) is chosen for the resonant frequency, one may use 68.800, 78.629, ... MHz for the nonresonant sidebands.

F. Achievable asymmetries

The optimum value of the Schnupp asymmetry depends strongly on the parameters of the interferometer (mirror reflectivities, beam splitter properties, *etc.*) so the Detector Subsystem Requirements document calls for a range of adjustment, over $S_s = 0$–250 mm.[4] I checked that this range was available for the chosen configurations. The actual range achievable is given in Table 7. In this calculation, it was assumed that both the position of the recycling mirror and the positions of the input test masses were adjusted.

Table 7. Achievable Schnupp asymmetries (in mm).

IFO	n, k	f_{res} (MHz)	Schnupp range	Limiting factor
4-km	2,1	24.493	-100 to +500	RC reaches maximum.
2-km	3,2	29.486	-100 to +300	RC reaches minimum.

G. Summary: frequencies and lengths

The resonant and nonresonant frequencies and lengths that satisfy the various constraints are listed in the following table.

Table 8. Optimized modulation frequencies for resonant sidebands and corresponding optical lengths (in mm).

IFO	n, k	f_{res} (MHz)	n'	f_{nr} (MHz)	L_{mc}	L_{rc}
4-km	2,1	24.493	5	61.232	12240	9188
2-km	3,2	29.486	7	68.800	15251	12715

References

1. M. Zucker and P. Fritschel, LIGO-T960122-00-I.
2. D.B. Tanner, 2 January 1997.
3. Dennis Coyne, "Recycling cavity and mode cleaner cavity baseline dimensions," LIGO-T970068-00-D
4. D. Shoemaker, "Detector Subsystem Requirements" LIGO-E960112-05-D, 23 August 1996.
5. Jordan Camp, David Reitze, and David Tanner, "Input/output optics conceptual design," LIGO-T960170-00-D, 1996.
6. Tom Delker, "Layout of HAM 7&8." (Preliminary, 27 May 1997).
7. L. Schnupp, 1987 (unpublished).
8. R. Flaminio and H. Heitmann, "Interferometer Locking Scheme," VIRGO Note PJT93021 (1993).
9. Jordan Camp, "Initial length precision of LIGO suspended cavities," LIGO-T960181.

BATCH START

STAPLE
OR
DIVIDER

LIGO-T970156-00-D

FAX MESSAGE FROM

UNIVERSITY OF FLORIDA

DEPARTMENT OF PHYSICS

Gainesville, Florida 32611-8440

FAX: (352) 392-3591
Voice: (352) 392-4718
Internet: tanner@phys.ufl.edu

Number of pages, including this page: 17

18 August 1997

FAX to:	Dennis Coyne
Number:	(818)304-9834
From:	David Tanner DMT
Subject:	Latest (last?) version of paper about lengths.

This has the numbers we used in the PDD.

Jordan's correction for the phase shift of the resonant sideband at the ITM's It is mentioned on p.9. This phase is uncertain at the 10% level for sure and possibly at the 50% level, so it doesn't make sense in my opinion to worry too much about the last few mm.

DT:dt

LIGO cavity lengths and modulation frequencies

D.B. Tanner

Department of Physics, University of Florida, Gainesville, FL 32611-8440, USA

The lengths of the mode cleaner (L_{mc}) and of the recycling cavity (L_{rc}) in LIGO are considered in light of constraints imposed by existing vacuum chamber dimensions. The optimum lengths, and corresponding modulation frequencies, are given in the following table. Here, f_{res} is the frequency of a modulation that produces sidebands resonant in the recycling cavity but not the interferometer arms. f_{nr} is the frequency of a modulation that is not resonant in either. Both sets of sidebands must resonate in the mode cleaner.

IFO	L_{mc} (mm)	L_{rc} (mm)	f_{res} (MHz)	f_{nr} (MHz)
4-km	12240	9188	24.493	61.232
2-km	15251	12715	29.486	68.800

Gainesville, 17 August 1997

TABLE OF CONTENTS

A. Introduction

This note is one of a series of memos about baseline lengths for the mode cleaner and recycling cavity, along with the corresponding RF modulation frequencies. The series includes work by M. Zucker and P. Fritschel,[1] myself,[2] and Dennis Coyne.[3] The baseline RF frequencies are listed in the Detector Subsystem Requirements[4] and in the IOO Conceptual Design document.[5] They are 24.0 MHz for the 4-km interferometer and 32.1 MHz for the 2-km interferometer.

In the current phase of the input optics (IOO) design these lengths and nominal frequencies are refined, as described in this note.

B. Relation between lengths and modulation frequencies

The core optics of LIGO employ two modulation frequencies:

1. The first modulation frequency gives upper and lower sidebands that are resonant in the recycling cavity but not resonant in the interferometer arm cavities. These are used for controlling the lengths of the interferometer and for aligning the arm cavities and the beam splitter.
2. The second gives upper and lower sidebands that are not resonant in the recycling cavity. These are used for alignment of the recycling mirror.

The values of these frequencies are set by the lengths of the respective cavities, according to the usual Fabry-Perot conditions.

The resonant sideband frequency must satisfy

$$f_{res} = \frac{(k+1/2)c}{2L_{rc}}, \tag{1}$$

where ($k = 0,1,2 \ldots$) and L_{rc} is the recycling cavity length. The extra factor of 1/2 occurs because the carrier is resonant in the arm cavities whereas the sidebands are *not* resonant in the arms, giving a extra 180° phase shift in the reflectivity of the arms.

The nonresonant sideband frequency is chosen to be far from the recycling cavity resonances. A reasonable condition is that the frequency offset be several times the width of the resonance, so that the phase shift on reflection be close to 0.

Both the resonant and nonresonant sidebands must be equal to one of the mode cleaner resonances, because the RF modulation is imposed before the mode cleaner. The resonant frequencies of the mode cleaner are:

$$f_{mc} = \frac{nc}{2L_{mc}}, \tag{2}$$

where n is an integer (1,2,3 ...) and L_{mc} the mode cleaner length.* The frequencies f_{mc} and f_{res} must equal each other because the sidebands are resonant simultaneously in both the mode cleaner and the recycling cavity.

The remaining consideration in choice of the modulation frequencies is that they must miss all the harmonics of the arm free spectral range: 37.5 kHz in the 4-km instrument; 75 kHz in the 2-km instrument.

C. Constraints affecting modulation frequencies

1. Vacuum chambers

The mode cleaner and recycling cavities span vacuum chambers whose separations determine the cavity lengths. There is some flexibility on account of the size of the optical tables in these chambers. The mode cleaner for the 4-km instrument occupies HAM-1 and HAM-2; the interferometer recycling mirror is in HAM-3; the input test masses are in BSC-1 and BSC-3. The mode cleaner for the 2-km instrument occupies HAM-7 and HAM-8; the recycling mirror is in HAM-9; the input test masses are in BSC-7 and BSC-8. Table 1 gives some details.

Table 1. Dimensions of vacuum chambers in LIGO, in mm.

Item			
	HAM table length, L_{HAM}	1905	
	HAM table width, W_{HAM}	1702	
	BSC table length,† L_{BSC}	931	
	BSC table width,† W_{BSC}	845	
IFO		Min	Max
Both	HAM-1(7) to HAM-2(8) (Mode Cleaners)	11816	15626
4-km	HAM-3 to BSC-1/3 (Recycling Cavity)	6890	9726
2-km	HAM-9 to BSC-7/8 (Recycling Cavity)	11530	14366

† The BSC tables are 1257 mm in diameter; I've taken the size as the included rectangle whose width is the distance between the outsides of the large optics suspensions (*LOS*) on these tables.

The Min and Max dimensions in Table 1 must be adjusted by several factors to estimate

* The length is ***half*** the round-trip length of the cavity. For a triangular-mode cleaner, in the shape of a tall isosceles triangle, it is then half the base plus the length from base corner to apex.

the minimum and maximum path lengths in mode cleaner and recycling cavities. These adjustments are listed in the following sections.

2. *Mode cleaner*

The mode cleaner is sketched in Fig. 1, with some key dimensions marked. The factors governing the optical length of the mode cleaner include the following items:

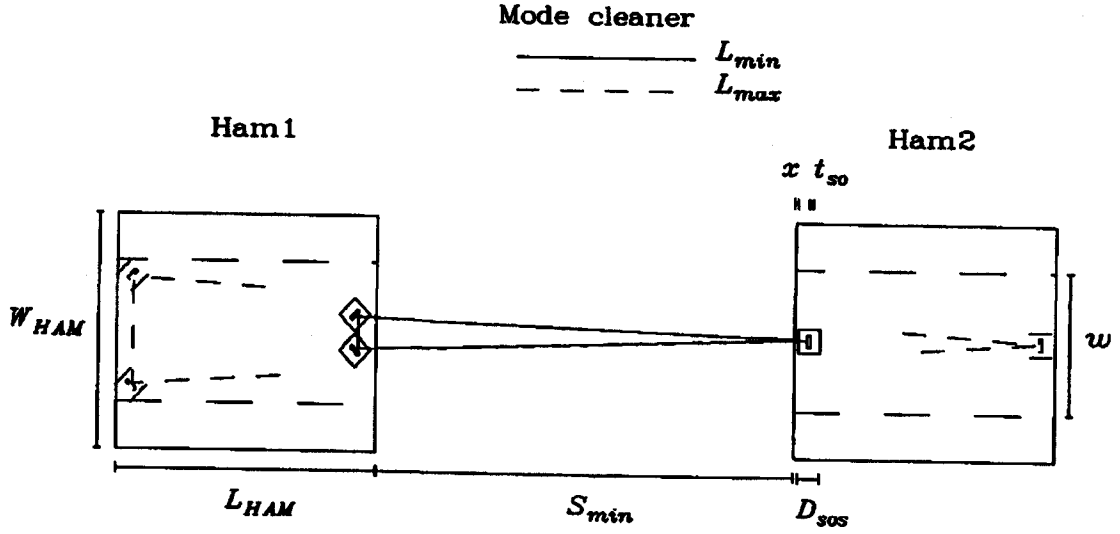

Fig. 1. The mode cleaner. The tables are shown approximately 4× enlarged in size, with the suspension bases and mirror thicknesses roughly to the scale of the tables. The minimum length is shown as the solid line; the maximum as dashed lines.

1. S^{mc}_{min} is the minimum table separation and S^{mc}_{max} is the maximum table separation, from Table 1.
2. The curved mirror must be moved away from the edge of the table so that the small optics suspension (*sos*) does not overhang the table. The distance from mirror face to table edge is half the depth of the suspension (D_{sos}) adjusted by half the thickness of the optic (t_{so}). (If the mirror is near the back edge—from its point of view—there must be space behind it for a length/alignment sensing pickoff. See point 7, below.)
3. The flat mirrors are at nearly 45° to the table edge, so their centers need to be moved away by $\sqrt{2}/2$ of D_{sos}, with an adjustment for the thickness of the mirror $[(\sqrt{2}/2)t_{so}]$.
4. The base b of the triangular beam path in the mode cleaner must be included in the optical path length. The minimum base size is set by having the corners of the small

optics suspension almost touching. It might seem that the maximum could be set by using the full 1702 mm width W_{HAM} of the HAM chamber table, less the $(\sqrt{2}/2)D_{sos}$ needed to keep each suspension fully on the table. However, the beam tube joining HAM-1 and HAM-2 is only 775 mm in diameter, and this tube also must accommodate the large beam from the IOO telescope. Thus, I have used half the tube diameter, 387 mm for the available width, w. (This also allows space on the HAM tables for beam expanders and steering mirrors.)

5. Both the minimum and the maximum size for b are adjusted for the thickness of the mirror.

6. There is another adjustment because the long sides of the triangular path are not parallel to the axis, and so are longer by approximately $b^2/8S$. This quantity is $\approx$1 mm when the base equals its maximum value, and even more negligible when the base is near its minimum.

7. The mode cleaner need a certain amount of space A_{ax} around it to allow for the extraction of auxillary beams. This distance includes space for a mirror behind the spherical mirror and for beam steering mirrors near the two flats.[6] This space takes away from the maximum length of the mode cleaner.

8. There probably should be a small gap x between the suspensions and between the actual table edge, in the cases where the suspensions approach the edge, to allow for chamfers or lips at the edge introduced by the machining process.

From the above, I arrive at the following equations for the effective optical path lengths in the mode cleaner.

Minimum:

$$L^{mc}_{min} = S^{mc}_{min} + \frac{1+2\sqrt{2}}{2}(D_{sos} - t_{so}) + 3x \tag{3}$$

Maximum:

$$L^{mc}_{max} = S^{mc}_{max} - \frac{1+2\sqrt{2}}{2}(D_{sos} + t_{so}) - 2A_{ax} - 2x + \frac{1}{2}w + \frac{w^2}{8S^{mc}_{max}} \tag{4}$$

3. Effect of Schnupp asymmetry and beam offsets

LIGO uses Schnupp or frontal modulation in its length-sensing and alignment system.[7,8] The basic idea is to introduce an asymmetry between the Michelson arms. When the carrier is exactly at a dark fringe, the modulation sidebands will be slightly away from a dark fringe, so that some sideband power is sent by the interferometer into the output port. This

power generates signals used in the beam splitter and input test mass locking scheme. The baseline design for LIGO uses an asymmetry* of $S_s = 250$ mm.[4] Finally, so far as the effective recycling cavity length for the RF modulation goes, it is the *average* length of the recycling cavity that matters.

Both the 4-km and the 2-km interferometer have their optical centerlines displaced from the centerlines of the beam tubes. Because of this offset, the placement of the beam splitter may affect the Michelson and recycling cavity path length by making a difference between the y optical path and the x optical path. It is possible to use this difference to minimize the impact of the Schnupp offset on the range of motion of the input test masses.

a. 4-km interferometer

The 4-km interferometer has its optical centerline displaced (by $B_{off} = 200$ mm) from the centerlines of the beam tubes. Because of this offset, the placement of the beamsplitter affects the Michelson and recycling cavity path length, as sketched in Fig. 2, below. In this figure, the x and y coordinates intersect at the center of the beamsplitter chamber. If the beamsplitter is in the second or fourth quadrant, the y physical length will be shorter or longer than the x physical length by $2B_{off}$. If the beamsplitter is in the first or third quadrant, the offset has no effect on length. In the present design, the beamsplitter is in

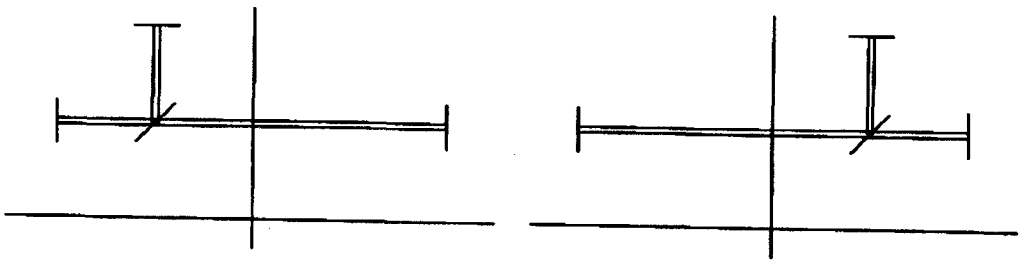

Fig. 2. Recycling cavity in the 4-km interferometer illustrating the effect of beamsplitter placement on Michelson optical path lengths. In each drawing the recycling mirror is on the left and the x and y input test masses are on the right and top, respectively. These are the same distance along the centerline from the origin. The beamsplitter is displaced from the origin; it in the second quadrant in the left drawing and the first quadrant on the right. The asymmetry in path lengths in the left drawing is evident.

* Note that there are three possible definitions for this quantity: (1) the optical path difference, (2) the difference in physical lengths, (3) the amount each mirror is moved from the equal-path-difference location. According to the Detector Subsystem Requirements document,[4] the maximum Schnupp distance of 250 mm refers to 1/2 the physical difference in lengths, *i.e.*, option (3) above. In this case, the optical path difference is 1 m.

the second quadrant, giving an asymmetry in the paths. The beam along x goes the same distance as if it were on the centerline; the beam along y turns a distance B_{off} before it reaches the y axis, and starts parallel to y from a point B_{off} above the x axis.

With the Schnupp offset included, the remaining asymmetry in placement of the input test masses is

$$A_{symm} = |B_{off} - S_s|. \tag{5}$$

(This is defined in the same way as the Schnupp offset, *i.e.*, as 1/2 the physical difference in lengths if the ITM's are placed in identical positions on the tables.)

b. 2-km interferometer The layout of the 2-km interferometer is shown in Fig. 3. This instrument also has its optical centerline displaced (by $B_{off} = 200$ mm) from the centerlines of the beam tubes. In addition, the 2-km interferometer is folded into the beam tubes by

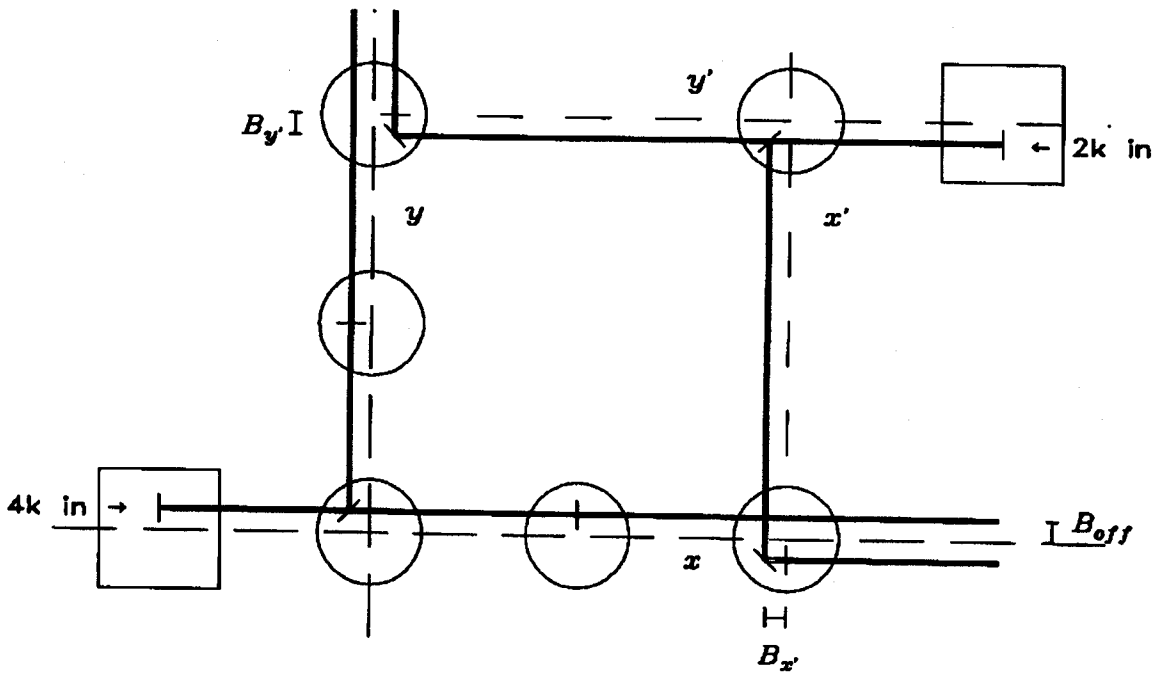

Fig. 3. Optical layout of the core optics. The coordinate systems are shown as dashed lines, crossing in the two beamsplitter chambers. Both interferometers have their beams offset from the centerline by B_{off}. The 2-km beam enters in the upper right. The 2-km beamsplitter directs the beam parallel to the x' and y' axes. The offsets $B_{x'}$ and $B_{y'}$ are shown. Turning mirrors direct the beam into the arm cavities. The recycling mirrors and input test masses are shown as small dashes, centered in their chambers.

turning mirrors located in the same BSC's as the input test masses. These turning mirrors have two consequences: (1) They take up space in the chamber, reducing the range of motion of the ITM's. (2) Their placement, coupled with the beamsplitter location, gives some additional adjustability in the x and y path lengths.

The 2-km interferometer has an asymmetry given by

$$A_{symm} = |B_{off} - B_{y'} + B_{x'} - S_s|, \tag{6}$$

where $B_{x'}$ and $B_{y'}$ are the offsets of the beams from the tube centerlines along the paths between the beamsplitter and the turning mirrors.

4. Recycling cavity

The recycling cavity is sketched in Fig. 4, with some key dimensions marked. The factors governing the optical length of the recycling cavity include the following items:

1. S_{min} is the minimum table separation and S_{max} is the maximum table separation, from Table 1.

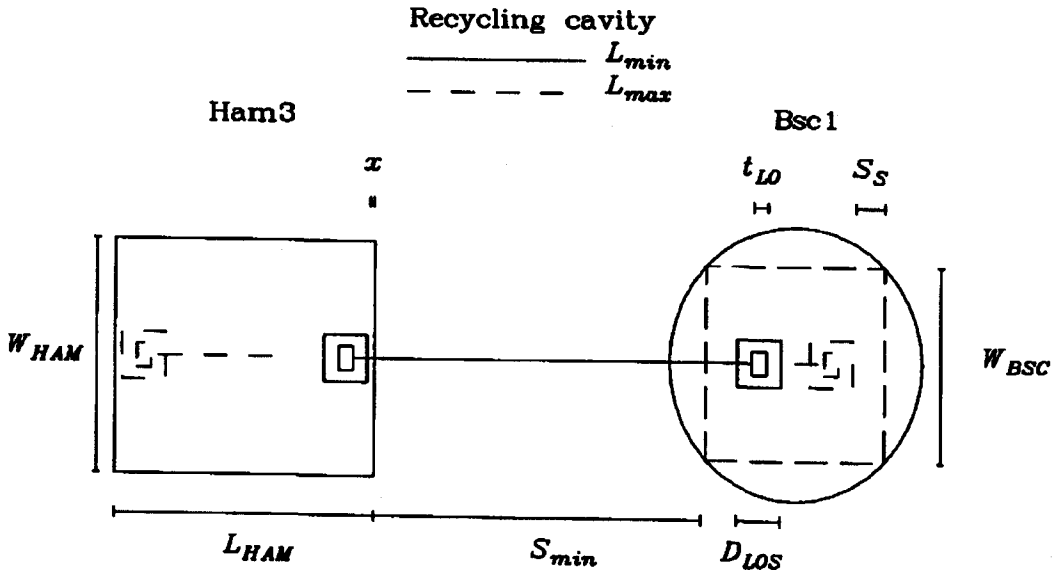

Fig. 4. The recycling cavity. The tables are shown approximately 4× enlarged in size with the suspension bases and mirror thicknesses roughly to the scale of the tables. The minimum length is shown as the solid line; the maximum as dashed lines. The Schnupp offset prevents the average location of the input test mass from being moved to the edges of the table.

2. The average position of the input test masses must be moved away from the table edge by the remaining asymmetry, which is given in Eqs. 5 and 6, above.
3. The mirrors must be moved away from the edge of the table so that the large optics suspensions (LOS) do not overhang the table. The distance from mirror face to table edge is half the depth of the suspension (D_{LOS}). Note that the recycling mirror faces the cavity, but the input test mass reflective surface faces *away* from the cavity, so that the offsets from the thickness of the optic cancel.
4. There needs to be an adjustment for the extra optical path in the substrate of the input test mass, $(n-1)t_{LO}$, where n is the refractive index.
5. There is also an adjustment for the additional path in the beam splitter (including the effects of refraction), δt_{BS}. With a little bit of trigonometry and Snell's law, I get the neat result

$$\begin{aligned} \delta t_{BS} &= t_{BS}\left(\sqrt{n^2-\sin^2\theta_i}-\cos\theta_i\right) \\ &= t_{BS}\left(\sqrt{n^2-\frac{1}{2}}-\sqrt{\frac{1}{2}}\right) \qquad \text{with } \theta_i = 45^\circ \end{aligned} \tag{7}$$

   where θ_i is the angle of incidence and t_{BS} the beam-splitter thickness.
6. There probably should be a small gap x between the suspensions and the actual table edge, to allow for chamfers or lips at the edge introduced by the machining process.
7. In the 2-km interferometer, space must be left for the turning mirrors. With a little geometry, I find that this increases the minimum path length by

$$F = \frac{L_{BSC}}{2} - \min(B_{x'}, B_{y'}) + \frac{D_{LOS} + W_{LOS} - t_{LO}}{\sqrt{8}}. \tag{8}$$

8. In the 4-km interferometer, of course, $F = 0$.

From this I come to the following equations for the effective optical path lengths in the recycling cavity.

Minimum:

$$L^{rc}_{min} = S^{rc}_{min} + A_{symm} + D_{LOS} + 2x + (n-1)t_{LO} + \delta t_{BS} + F \tag{9}$$

Maximum:

$$L^{rc}_{max} = S^{rc}_{max} - A_{symm} - D_{LOS} - 2x + (n-1)t_{LO} + \delta t_{BS} \tag{10}$$

D. Arm resonances

I have considered briefly the interrelation of the arm-cavity resonances and the recycling cavity resonances. The arm-cavity resonances occur at:

$$f_{arm} = \frac{\ell c}{2L_{arm}}, \tag{11}$$

where $L_{arm} = \{4, 2\}$ km and ℓ is an integer. The frequency separation of these resonances is 37.5 kHz for the 4-km interferometers, and 75 kHz for the 2-km interferometer. When the length of the arms is resonant with the carrier signal, the sidebands must fail to resonate in the arms, *i.e.*, $f_{res} \neq f_{arm}$. However, the arms should not be maximally antiresonant, in order to keep the second-order sidebands from resonating in the arm cavities.[9] I have adjusted the calculations below to move the modulation frequencies 4–6 kHz away from the maximmally antiresonant values. Typically, to make the arm cavities adequately nonresonant requires a length change of about 2 mm in the mode cleaner and recycling cavity lengths, and changes the resonant modulation frequency by a few kHz. Note that it takes a length change of about 6000 mm in arm-cavity length to move the sidebands from the ℓ^{th} arm resonance to the $\ell \pm 1^{\text{st}}$ arm resonance. Since 3m of motion is probably not available in the positioning of the test masses, it will most likely be the responsibility of the mode-cleaner and recycling cavities to avoid degeneracy with the arm cavities.

Displacement of the arm cavities from antiresonance leads to a phase change in the reflected sidebands $\Delta\phi$. This value is estimated in LIGO-T960181[9]; it is typically 0.01 radians. In turn, the recycling cavity must be increased in length by $\Delta\phi L_{rc}/(2k+1)\pi$, a value of 5–8 mm.

E. Numerical values

1. Dimensions used

Table 2 lists the quantities that come into the calculation and gives the values used. Using these numbers, I calculate the *optical lengths* for the interferometers, in Table 3. The range of lengths in Table 3 is somewhat less than those in Table 1.

2. Resonant sideband frequencies

Given the above range of lengths, it is then possible to find the range of frequencies for which *both* the mode cleaner and the recycling cavity resonance conditions (Eqs. 2 and 1) are satisfied. Several candidate length and modulation frequency ranges emerge. These are listed in Table 4, which should be compared to Table 3 of Ref. 1.

I also carried out an optimization in Excel to (1) adjust the mode cleaner length within the limits given in Table 3, (2) calculate the corresponding recycling cavity length, (3)

Table 2. Quantities affecting the optical lengths of the mode cleaner and recycling cavities. (All dimensions in mm.)

Item	Symbol	Value
Small optic suspension depth	D_{sos}	127
Small optic suspension width	W_{sos}	156
Small optic thickness	t_{so}	25
Space for auxillary mirrors	A_{ux}	105
Edge clearance	x	10
Beam tube limits on MC width	w	387
Large optic suspension depth	D_{LOS}	267
Large optic suspension width	W_{LOS}	445
Large optic thickness	t_{LO}	100
Beam-splitter thickness	t_{BS}	40
Offset in beam tube	B_{off}	200
2-km x' offset	$B_{x'}$	57
2-km y' offset	$B_{y'}$	161
Schnupp offset (nominal)	S_s	250
Schnupp offset (maximum, 4k)	S_s^{4k}	500
Schnupp offset (maximun, 2k)	S_s^{2k}	300
Turning mirror space in 2-km IFO	F	604
Refractive index	n	1.45

Table 3. Optical lengths in LIGO, in mm.

IFO		Min	Ave	Max	Range of motion
Both	Mode cleaner	12041	13671	15300	3259
4-km	Recycling cavity	7444	8375	9306	1862
2-km	Recycling cavity	12663	13327	13992	1329

assure that the recycling cavity was within limits, (4) optimize the lengths to center them within the allowable range, and (5) make small adjustments in length to make the resonant sideband adequately nonresonant in the arm cavities. This procedure leads to the suggested frequencies in Table 5, which should be compared to Table 1 of Ref. 3.

Table 4. Bounds for the 4k and 2k interferometers up to $n = 5$, $k = 5$. (All dimensions in mm.)

IFO	n,k	L_{mc}/L_{rc}	f (MHz)	L_{mc}	L_{rc}
4-km	1,0	2.0	9.80–10.07	14889–15300	7444–7650
	2,1	1.3333	24.16–24.90	12041–12408	9031–9306
	3,1	2.0	29.39–30.20	14889–15300	7444–7650
	4,2	1.6	40.27–49.80	12041–14889	7526–9306
	5,2	2.0	48.98–50.34	14889–15300	7444–7650
	5,3	1.4286	56.38–62.24	12041–13294	8429–9306
2-km	3,2	1.2	29.39–29.59	15196–15300	12663–12750
	4,3	1.1429	39.19–41.43	14472–15300	12663–13388
	4,4	0.8889	48.21–49.80	12041–12437	13546–13992
	5,4	1.1111	48.98–53.27	14070–15300	12663–13770
	5,5	0.9091	58.92–62.24	12041–12437	13245–13992

Table 5. Optimized modulation frequencies for resonant sidebands and corresponding optical lengths. (All dimensions in mm.)

IFO	n,k	Notes	f (MHz)	L_{mc}	L_{rc}
4-km	1,0	MC length 2× RC.	9.886	15163	7582
	2,1		24.569	12202	9152
	3,1	MC length 2× RC.	29.657	15163	7582
	4,2	Recycling mirror centered in chamber.	44.745	13400	8375
2-km	3,2		29.498	15245	12704
	4,3		40.204	14914	13050
	4,4		48.943	12251	13782

Several comments may be made about Tables 4 and 5:

1. Given the constraints I have used, it is not possible to get a 24.0 MHz modulation frequency for the 4-km interferometer.
2. Neither is there a solution at 32.1 MHz for the 2-km configuration.
3. The solutions $n,k = 2,1$, with frequency 24.569 MHz (4-km), $n,k = 3,2$, with frequency 29.498 MHz (2-km), correspond to the n,k parameters chosen in Refs. 1 and 3.
4. The 2-km interferometer has no solution below 28.391 MHz, although there is a close match at $n,k = 2,1$ at 18.67 MHz frequency.

5. The $n, k = 1, 0$ and $n, k = 3, 1$ solutions for the 4-km interferometer, although good from the point of view of length flexibility are probably ruled out by the wish to avoid integer ratios of lengths.

6. From the point of view of the optical layout, the mode cleaner prefers to be a little bit larger (say 500 mm larger) than its minimum size. (If it is right at either extreme, there is no chance to play off base size with height; if it tends towards its maximum size, it eats up real estate in HAM-1.)

3. Comparison to LIGO-T970068-00-D

As already mentioned, the $n, k = 2, 1$ (4-km) and $n, k = 3, 2$ (2-km) correspond to the n, k parameters chosen in Refs. 1 and 3. The first two lines of Table 6 compares the numbers in Table 5 with those in Ref. 3. The results are very close.

The lengths in Ref. 3 were obtained graphically using a CAD program, and there were no constraints that the modulation frequencies be antiresonant with the arm cavities. The third line shows the modification to those lengths if this constraint is imposed. The freqeuncies are changed by about 30 kHz (4-km) and 37 kHz (2-km) when this is done, with corresponding changes in length. I recommend choosing these values for the instrument.

Table 6. Comparison with previous results for frequencies and lengths. (All dimensions in mm.)

IFO	n, k	Notes	f (MHz)	L_{mc}	L_{rc}
4-km	2,1	LIGO-T970068-00-D	24.463	12255	9191
	2,1	Table 5	24.569	12202	9152
	2,1	Reoptimized LIGO-T970068-00-D	24.493	12240	9188
2-km	3,2	LIGO-T970068-00-D	29.449	15270	12725
	3,2	Table 5	29.498	15245	12704
	3,2	Reoptimized LIGO-T970068-00-D	29.486	15251	12715

4. The nonresonant sidebands

One has not a lot of flexibility with regard to the nonresonant sidebands. They must satisfy Eq. 2 but with a *different* mode cleaner resonance, $n' \neq n$. Moreover, in order to reduce the effects of "sidebands on sidebands" associated with series phase modulation of the laser, the nonresonant sidebands should be as large as possible compared to the resonant sidebands, at least $> 2\times$ them. Finally, because the Pockels cell produces harmonics at multiples of the modulation frequency, integer ratios of frequencies should be avoided.

a. 4-km interferometer

If 24.569 MHz ($n = 2$) is chosen for the resonant sideband frequency, one may in use 61.232, 85.725, 110.218 ... MHz for the nonresonant sidebands. This leads to 61.232 MHz ($n' = 5$) as the likely nonresonant sideband modulation frequency.

b. 2-km interferometer

If 29.498 MHz ($n = 3$) is chosen for the resonant frequency, one may use 68.800, 78.629, ... MHz for the nonresonant sidebands.

F. Achievable asymmetries

The optimum value of the Schnupp asymmetry depends strongly on the parameters of the interferometer (mirror reflectivities, beam splitter properties, *etc.*) so the Detector Subsystem Requirements document calls for a range of adjustment, over $S_s = 0$–250 mm.[4] I checked that this range was available for the chosen configurations. The actual range achievable is given in Table 7. In this calculation, it was assumed that both the position of the recycling mirror and the positions of the input test masses were adjusted.

Table 7. Achievable Schnupp asymmetries (in mm).

IFO	n, k	f_{res} (MHz)	Schnupp range	Limiting factor
4-km	2,1	24.493	-100 to +500	RC reaches maximum.
2-km	3,2	29.486	-100 to +300	RC reaches minimum.

G. Summary: frequencies and lengths

The resonant and nonresonant frequencies and lengths that satisfy the various constraints are listed in the following table.

Table 8. Optimized modulation frequencies for resonant sidebands and corresponding optical lengths (in mm).

IFO	n, k	f_{res} (MHz)	n'	f_{nr} (MHz)	L_{mc}	L_{rc}
4-km	2,1	24.493	5	61.232	12240	9188
2-km	3,2	29.486	7	68.800	15251	12715

References

1. M. Zucker and P. Fritschel, LIGO-T960122-00-I.
2. D.B. Tanner, 2 January 1997.
3. Dennis Coyne, "Recycling cavity and mode cleaner cavity baseline dimensions," LIGO-T970068-00-D
4. D. Shoemaker, "Detector Subsystem Requirements" LIGO-E960112-05-D, 23 August 1996.
5. Jordan Camp, David Reitze, and David Tanner, "Input/output optics conceptual design," LIGO-T960170-00-D, 1996.
6. Tom Delker, "Layout of HAM 7&8." (Preliminary, 27 May 1997).
7. L. Schnupp, 1987 (unpublished).
8. R. Flaminio and H. Heitmann, "Interferometer Locking Scheme," VIRGO Note PJT93021 (1993).
9. Jordan Camp, "Initial length precision of LIGO suspended cavities," LIGO-T960181.